Jurnal Teknologi

Full Paper

EVALUATION OF INTERMOLECULAR INTERACTION OF CALCIUM CARBONATE, BARIUM SULPHATE AND IRON (II) SULFIDE SOLID DISSOLUTION IN DTPA AND EDTA

Muhamad Hadi Sulaiman[a]*, Fatmawati Adam[b], Navinesh Nedumaran[b], Jennifer Selvarajan[b], Waigesh Kessevan[b]

[a]UTMSPACE, Universiti Teknologi Malaysia, 54100, Kuala Lumpur, Malaysia
[b]Faculty of Chemical and Process Engineering Technology, Universiti Malaysia Pahang Al-Sultan Abdullah, Kuantan, Pahang, Malaysia

Article history
Received
17 September 2024
Received in revised form
23 December 2024
Accepted
12 February 2025
Published Online
24 October 2025

*Corresponding author
hadi@utmspace.edu.my

Graphical abstract

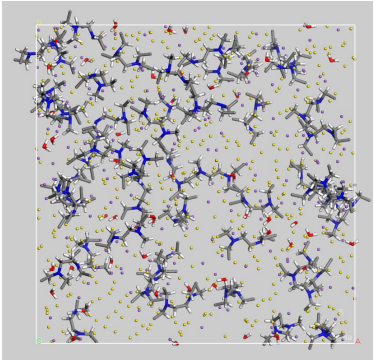

Abstract

In this work, formulations for dissolution of calcium carbonate (CaCO3), barium sulphate (BaSO4) and iron (II) sulphide (FeS) were developed. Tri potassium EDTA (EDTA-K3), tetrasodium EDTA (EDTA-Na4) and pentapotassium DTPA (DTPA-K5) were blended with synergist to dissolve CaCO3, FeS and BaSO4 solids respectively. The synergists used are hydrochloric acid (HCl) and acetic acid (HAc) for CaCO3, potassium carbonate (K2CO3) for BaSO4 and formic acid for FeS. Molecular dynamic simulations were conducted to study the intermolecular interaction (g(r)) between oxygen in the chelating agent with the metal ion in the solid scale. The (g(r)) of oxygen in EDTA-K3 with Ca shows an increment from 6.06 to 6.86 at a radius (r) of 2.25 Å with the addition of a synergist. However, g(r) of Ba with oxygen in DTPA-K5 shows reduction with the addition of synergist from 2.68 to 1.40 at r of 3.25 Å. The g(r) of Fe with oxygen in EDTA-Na4 also shows reduction with the addition of synergist from 10.7 to 10.01 at r 1.75 Å. Overall, the g(r) of Fe and Ca with respective chelate agents was good, while Ba was weak. The dissolution test at 60 °C for 24 hours was performed and validated with ICP-OES. The blending formulation dissolved 68 % mass of CaCO3 (19 940 ppm Ca), 40 % of BaSO4 (8 200 ppm Ba), and 25% of FeS (3 528 ppm Fe). The findings useful to give insight into the synergist chemical role at the nanoscale in chelating the metal is solid scale dissolution.

Keywords: Chelate agent, intermolecular interaction, solid scale dissolution, EDTA, DTPA

Abstrak

Dalam kajian ini, satu formulasi untuk pelarutan kalsium karbonat (CaCO3), barium sulfat (BaSO4) dan ferum (II) sulfida telah dibangunkan menggunakan. EDTA tri kalium (EDTA-K3), EDTA tetra natrium (EDTA-Na4), dan DTPA penta kalium (DTPA-K5) telah di campur dengan bahan sinergis untuk melarutkan masing-masing pepejal CaCO3, FeS dan BaSO4. Sinergi yang digunakan adalah asid hidroklorik (HCl) dan asid asetik (HAc) untuk CaCO3, kalium karbonat (K2CO3) untuk BaSO4 dan asid formika untuk FeS. Simulasi dinamik molekul telah dijalankan untuk mengkaji interaksi antara molekul (g(r)) oksigen dalam agen pengelat dengan ion logam dalam pepejal tersebut. Didapati, (g(r)) oksigen dalam EDTA-K3 dengan Ca menunjukkan peningkatan daripada 6.06 kepada 6.86 pada jejari (r) 2.25 Å dengan penambahan sinergi. Walau bagaimanapun, g(r) molekul Ba dengan oksigen dalam DTPA-K5 menunjukkan pengurangan dengan penambahan sinergis daripada 2.68 kepada 1.40 pada r 3.25 Å.

g(r) Fe dengan oksigen dalam EDTA-Na4 juga menunjukkan pengurangan dengan penambahan sinergis daripada 10.7 kepada 10.01 pada r 1.75 Å. Secara keseluruhan, interaksi antara molekul Fe dan Ca dengan agen pengelat masing-masing adalah baik manakala interaksi Ba adalah lemah. Ujian kelarutan telah dijalankan pada suhu 60 °C selama 24 jam dan telah telah disahkan dengan ICP-OES. Formulasi campuran ini melarutkan 68% jisim CaCO3 (19 940 ppm Ca), 40% BaSO4 (8 200 ppm Ba), dan 25% FeS (3 528 ppm Fe). Hasil penemuan ini menyumbang pemahaman peranan bahan kimia sinergis pada skala nano dalam pengelatan logam dalam kerak pepejal.

Kata kunci: Agen pengelat, interaksi antara molekul, pelarutan kerak pepejal, EDTA, DTPA

1.0 INTRODUCTION

Calcium carbonate ($CaCO_3$), barium sulphate ($BaSO_4$) and iron (II) sulphide (FeS) are among the common solid scales deposition which occurs in oil well operation [1]. These scales can form in the perforations tunnel of the reservoir, which leads to the formation damage at the subsurface and surface of production facilities with major operational issues [2, 3]. Hydrochloric acid (HCl) is commonly used to dissolve solid scale, but its dissolution capability is limited to the type of scale [4] as well as corrosive [5], expensive when used in high-temperature stimulation as extra equipment and protection needed and may cause the release of toxic gas such as hydrogen sulphide [6, 7] from reaction with sulphur in oil well [4, 8]. Meanwhile, organic acids such as acetic acid and formic acid are used to reduce the corrosion properties but offer lower dissolution than HCl [9]. Also, organic and HCl acids can be combined to enhance the dissolution process and formulation [4]. Aminopolycarboxylic acid (APC) chelating agents effectively dissolve calcite at a low pH and cause the least damage to steel well tubular than mineral or organic acids [10, 11]. Amino acid ionic liquid has also been suggested as a potential chemical solvent for solid-scale dissolution, although still in early study [12]. Other than ionic liquid, a new generation solvent, which is a deep eutectic solvent, less toxic and greener, can be explored as a chelating agent for the solid scale dissolution [13]. The most common APCs are ethylenediaminetetraacetic acid (EDTA), hydroxyethylethylene diaminetriacetic acid (HEDTA), diethylenetriaminepentaacetic acid (DPTA) and nitrilotriacetic acid (NTA) which are used as metal ion chelates. The combinations of APC with acids are commonly used to prevent iron precipitation during acidising in oil wells, and the formulation can be used as a scale dissolver for $CaCO_3$ and FeS scales. EDTA deprotonates to H_2EDTA^{-2} and H_2EDTA^{-3}, which will participate in chelating calcium ions from calcium carbonate [14]. An increase in the concentration of EDTA in the solution contributes to an increase in the chelation site. Also, increasing EDTA concentration will reduce the active acetic acid sites due to decreasing solubility [15, 16]. Meanwhile, a synergist catalyst can also be used to dissolve the $BaSO_4$ scale. In the present work, a versatile EDTA and DTPA were developed to dissolve $CaCO_3$, $BaSO_4$ and FeS.

Intermolecular interaction between selected functional groups in a chelating agent with metal ions can provide insight at a molecular level of strength and probability of interaction that might form [12, 17, 18]. This interaction can be compared with experimental results to construct a possible relation between simulated intermolecular interaction and real situations. To study the intermolecular interaction between oxygen in the chelating agent with the metal ion in the solid scale, intermolecular interaction was simulated using molecular dynamic simulation and represented using radial distribution function (RDF). The RDF value, *g(r)*, gives the probability of finding an atom or molecule at a distance *r* from another atom or molecule compared to an ideal gas distribution; *g(r)* is dimensionless [19]. A closer interatomic distance (*r*) and higher peak (*g(r)*) can be interpreted to indicate a stronger interaction [20]. The RDF was generated for oxygen atoms in the carboxylic groups of the chelating agent with the metal ions in the solid scale as it will be the ligand that binds the metal ion [21]. Due to the tendency to form a bond and coulombic non-bonded interaction, the intermolecular interaction of the carboxyl group is expected to be high [18, 22].

2.0 METHODOLOGY

2.1 Molecular Dynamic Simulation

In this study, intermolecular interaction was simulated using molecular dynamic simulation, carried out using Material Studio version 7.0, licensed by Acceryls Inc (San Diego, USA). The workstation used to conduct this simulation was an HP Z400 workstation fitted with an 8 GHz dual-core processor running on Windows 7, 64-bit version. The molecular structure used in this study was downloaded from the database ChemSpider in a Jmol. format, which is supported by Material Studio [23]. Prior to the simulation, the structures were optimised, and the system for the interaction between solid scale and solvent was constructed using the Amorphous Cell

Box module. The dynamic simulation was conducted for constant NVE for 100ps. This was followed by dynamic simulation under constant NVT for another 900 ps to complete full 1ns of simulation time [12, 18, 24, 25]. The result was then analysed using the radial distribution function (RDF). The main functional groups that interact with a solid scale were oxygen in carboxylic (-COOH) or carboxylate ($-COO^-$). Oxygen was selected as the interaction site of interest due to the nature of the chelating agent forming a bond with metal ions using oxygen in the carboxyl group [12, 18, 26, 27]. Table 1 below shows the list of molecular dynamic simulation systems conducted in this study. The ratio of chelating agent with solid scale was chosen based on the capability of the chelating agent to form a bond with metal ions of at least a 1:1 molar ratio [28, 29]. The amount of water was estimated based on the optimum concentration of chelating agent previously reported in various literature [12, 18, 30, 31]. The selection of chelating agents and synergists for specific solid scales is based on the literature [17, 32-35]. Figure 1 shows the molecular structure of the chelating agent used in the intermolecular interaction simulation.

Table 1 Molecular dynamic simulation systems conducted with the number of molecules used of water, chelate, synergist and solid scale

System (Chelate--Solid Scale)	Number of Molecules			
	Water	Chelating Agent	Solid Scale	Synergist
EDTA-K_3--Calcium Carbonate	450	50	50	None
EDTA-K_3--Calcium Carbonate with Synergist (HCl)	450	50	50	17
DTPA-K_5--Barium Sulphate	450	50	50	None
DTPA-K_5--Barium Sulphate with Synergist (K_2CO_3)	450	50	50	17
EDTA-Na_4—Iron (II) Sulphate	450	50	50	None
EDTA-Na_4—Iron (II) Sulphate with Synergist	450	50	50	17

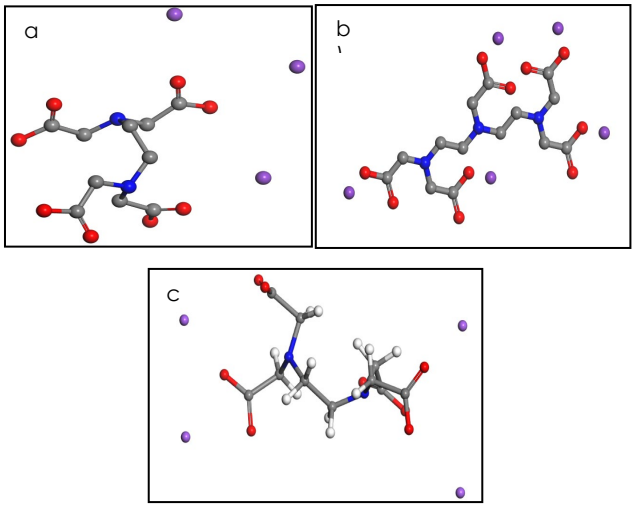

Figure 1 Molecular structure of chelating agents used in the intermolecular interaction simulation study a) EDTA-K_3, b) DTPA-K_5 and c) EDTA-Na_4 [23]

2.2 Chemicals and Materials

EDTA, EDTA-Na_4 (tetrasodium EDTA) and DTPA powder were purchased from Acros Organics. Hydrochloric acid (37 wt % HCl), Glacial acetic acid (99 wt % HAc), formic acid (98 wt %), potassium hydroxide (99.99 % KOH) pellets, potassium chloride (99.9 % KCl), potassium citrate, potassium carbonate (99.9 % K_2CO_3) and oxalic acid were used in the formulations. $CaCO_3$, $BaSO_4$ anhydrous and FeS (80%) were purchased from HmbG.

2.3 Formulation of Chemical Dissolver

Chemicals selected for dissolver formulation were based on the molecular dynamic simulation system listed in Table 1. Two or more chemicals were blended to study different scale solubility at different concentrations or amounts of synergist used. The chelating agent was first dissolved in deionised (DI) water in a beaker with a magnetic stirrer at medium speed. Synergist was then added slowly based on the desired concentration or amount into the chelate agent solution to avoid reprecipitation of the chelate agent. The solutions were transferred into a 250 ml volumetric flask to complete the preparation. Table 2 below shows the chelate agent and synergist used in the formulation for the selected solid scale. The selected solid scales were calcium carbonate ($CaCO_3$), Barium sulphate ($BaSO_4$) and iron (II) sulphide (FeS).

Table 2 Chelate agent and synergist use for selected solid scale

Chelate Agent	Synergist	Targeted Solid Scale
EDTA-K_3	HCl and HAc	$CaCO_3$
DTPA-K_5	K_2CO_3	$BaSO_4$
EDTA-Na_4	Formic Acid	FeS

2.4 Dissolution Test

The dissolution test was conducted using the gravimetric method at 60 °C for 24 hours with 4g of $CaCO_3$, 2g of $BaSO_4$ and 2g of FeS in different dissolver formulations. The sample was put into separate centrifuge tubes with 40 ml of formulation added [10-12]. A minimum of three repetitions were conducted to obtain an average and consistent dissolution percentage. Two of the formulation solutions after the dissolution test were selected for analysis using inductively coupled plasma optical emission spectroscopy (ICP-OES) analysis to identify the dissolved solid scale concentrations. The two solutions are among the highest dissolution tests for every dissolver formulation.

2.5 Properties Characterisation

2.5.1 Density Measurement

The desired dissolver solutions for every solid scale were determined after the dissolution test. The pH was measured using the Mettler Toledo pH meter. The density of the dissolvers was estimated using a pycnometer bottle and analytical balance. The mass of the liquid in a fixed volume at room temperature (25 ^{0}C) and pressure were measured repeatedly to obtain the mean value, and the density was calculated by dividing mass by volume [36, 37].

2.5.2 Boiling Point Analysis

The boiling point test was conducted using Buchi's melting point M-560 based on the Siwoloboff method [38]. The sample was placed into the heating block with the initial set temperature of 60 ^{0}C and heating rate of 10 ^{0}C/min until reaching a maximum temperature of 160 ^{0}C.

2.5.1 Corrosion Test

The corrosion test was conducted using the Gamry instrument interface 1000E, which was set up using the linear polarisation method (LPR) and carbon steel coupon as test material. The polarisation resistance method was selected with a scan rate of 0.125 mV/s with the potential range from ±10 mV [39].

3.0 RESULTS AND DISCUSSION

3.1 Intermolecular Interaction of EDTA with Calcium Carbonate

Figure 2 shows the intermolecular interaction of oxygen in EDTA-K_3 with calcium ions. At g(r) equal to 2.25 Å, the probability of interaction is computed at 6.06, showing a good intermolecular interaction between the chelation site in EDTA with calcium ions. The addition of synergists into the system improves the intermolecular interaction to probability g(r) at 6.86. In comparison, a previous study involving intermolecular interaction of the chelating agent with $CaCO_3$ shows intermolecular interaction simulated between oxygen atom in GLDA-NA_4 and DTPA-K_5 with calcium atom in $CaCO_3$ at g(r) equal to 2.25 Å is 4.19 [18] and 10.09 [35] respectively. In addition, Che Azimi, *et al*. [17] also reported that simulation of intermolecular interaction between DTPA with $CaCO_3$ occurs with a low probability of only 1.47.

Octadentate DTPA is one of the chelate agents with ligand sites, such as five carboxylic acids and three amine groups. DTPA, without its salt present as the functional group, is not suitable to bind $CaCO_3$ due to the low intermolecular interaction established, albeit the hydroxyl group has a strong intermolecular interaction with $CaCO_3$ [17]. Coulomb non-bonded might increase the interaction of the hydroxyl group with adjacent molecules [22]. Results from this study and previous studies indicate that the number of chelation sites and the presence of salt in the chelating agent functional group will improve intermolecular interaction between metals and the chelating agent. Strong intermolecular interaction from the simulation result in Figure 2 shows that EDTA-K_3 is a good and potential chelating agent to be used in the formulation of calcium carbonate scale dissolver.

The initial and final configuration of molecules for EDTA-K_3 with $CaCO_3$ is shown in Figure 3 without synergist and Figure 4 with synergist. Despite the good intermolecular interaction simulated, very few changes between the initial and final molecule configuration can be observed. This is due to more simulation time and an increased number of molecules considered in the simulation box for a better snapshot frame difference [40]. However, uniform distribution of the molecules can be observed in Figure 4 due to the addition of synergists in comparison to Figure 3, likely contributing to stronger intermolecular interaction as shown in Figure 2.

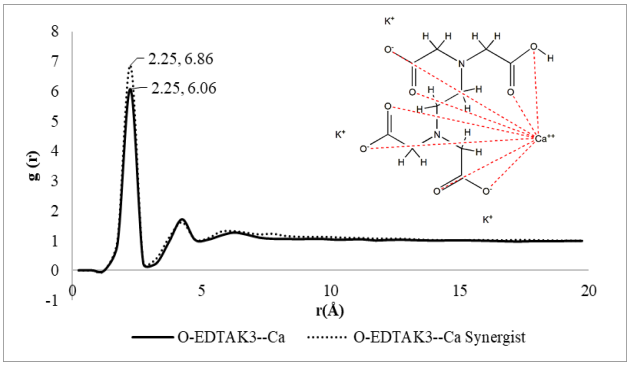

Figure 2 Intermolecular interaction of oxygen in EDTA-K_3 with calcium atom in $CaCO_3$ with and without synergist

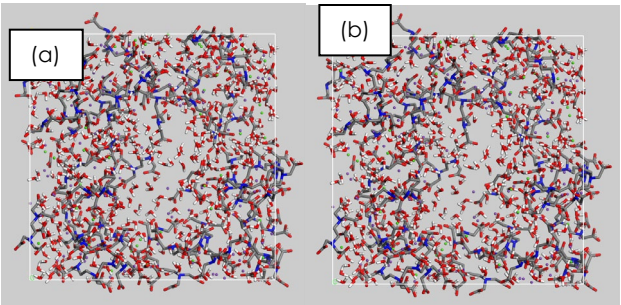

Figure 3 Initial (a) and final (b) configuration of molecules in EDTA-K_3--$CaCO_3$ system

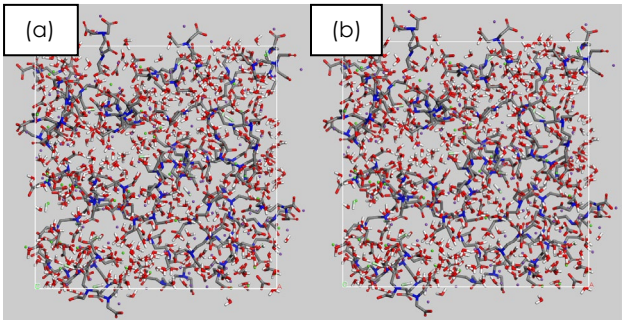

Figure 4 Initial (a) and final (b) configuration of molecules in EDTA-K_3--$CaCO_3$ with synergist system

3.1.2 Dissolution of Calcium Carbonate in EDTA-K3-Based Dissolver

Figure 5 shows the dissolution rates of $CaCO_3$ at 0.4 M, 0.5 M, and 0.6 M K_3-EDTA at 60 °C for 24 hours. Increasing the concentration of EDTA resulted in the increasing dissolution rate of $CaCO_3$ from 29% to 48% occurs at pH > 6.2. EDTA deprotonates to H_2EDTA^{-2} and H_2EDTA^{-3}, which will participate in chelating calcium ions from calcium carbonate [14]. An increase in the concentration of EDTA in the solution contributes to an increase in the chelation site. Also, increasing EDTA concentration will reduce the active acetic acid sites due to decreasing solubility [16]. Based on Figure 5, 0.6 of M K_3-EDTA was selected as the optimum concentration for the addition of HCl and acetic acid.

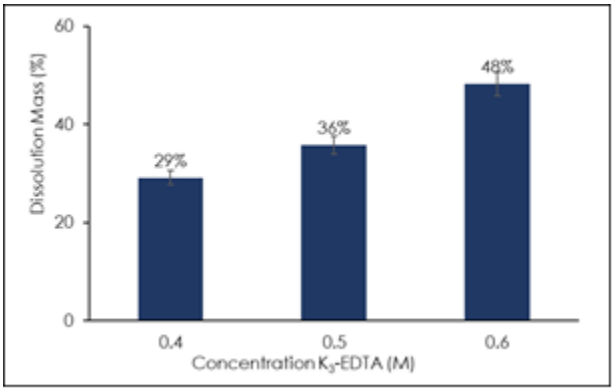

Figure 5 Dissolution of $CaCO_3$ in K_3-EDTA Solution

The addition of HCl as a synergist reduces the pH of the dissolver to 5.2-5.8. The reduction of pH contributes to the increase of the dissolution, as shown in Figure 6, with the highest dissolution achieved up to 58% with the addition of 0.2 M HCl at pH 5.6. This is because acetic acid is an organic acid that will be partially ionised in an aqueous solution, whereas HCl is a strong mineral acid that will be fully dissociated. Vigorous bubbling was observed during the initial process of dissolution, indicating the release of CO_2 gas [41]. EDTA slowly precipitates upon the addition of 0.5 M HCl due to a decrease in the pH of the solution. Previous studies showed that EDTA solution will precipitate at a pH below 4 [10, 42]. The usage of a low concentration of HCl (0.2 M) will reduce the corrosivity of the blending relative to using a high concentration of HCl.

Figure 7 shows the dissolution of $CaCO_3$ in 0.6 M K_3-EDTA with different concentrations of HAc (M). The highest dissolution of $CaCO_3$ was recorded up to 59%, with the addition of 0.3 M of HAc occurring at pH 5.9. This dissolution of $CaCO_3$ in EDTA-Hac is equally efficient as the EDTA-HCl blend (Figure 6). The addition of HCl or HAc to EDTA reduces the pH and increases the dissolution rate. This is due to more participation of hydrogen protons in the acid attack prior to chelation from EDTA molecules [41]. The efficacy of calcium chelation using EDTA depends on the solvent's pH to dissolve $CaCO_3$. Further formulation was made with the addition of both HCl and HAc into 0.6 M K_3-EDTA, as shown in Figure 8. The highest dissolution of $CaCO_3$ was recorded up to 68% for the addition of 0.2 M HCl and 0.3M HAc into 0.6 M K_3-EDTA, occurring at pH 4.87. ICP-OES analysis of the solvent after dissolution shows that calcium ions were dissolved up to 19 940 ppm. This calcium ions concentration result was on par with the commercial chelating agent-based dissolver previously reported by LePage *et al.*, [42] at 19 700 ppm at pH 3.0.

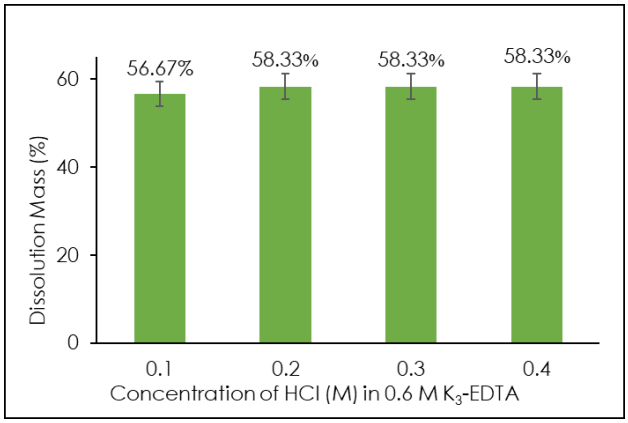

Figure 6 Dissolution of $CaCO_3$ in 0.6 M K_3-EDTA with different concentrations of HCl added

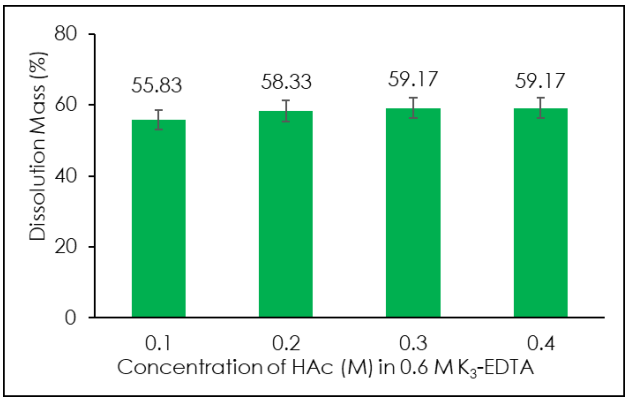

Figure 7 Dissolution of $CaCO_3$ in 0.6 M K_3EDTA with different concentrations of Hac (M)

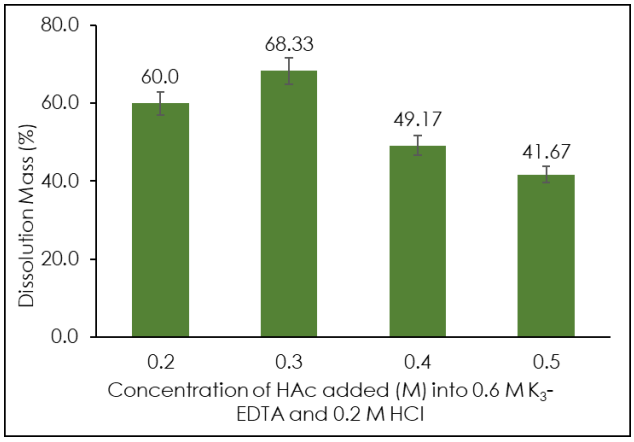

Figure 8 Dissolution of $CaCO_3$ in 0.6 M K_3-EDTA and 0.2 M HCl with different HAc (M) concentrations added

3.2 Intermolecular Interaction of DTPA with Barium Sulphate

Barium sulphate is considered as one of the most difficult solid scales to dissolve [30, 31]. However, DTPA-based solid scale dissolvers have been known to be effective when dissolving barium sulphate. Molecular dynamic DTPA-K_5 with barium in $BaSO_4$ was simulated. Figure 9 shows the intermolecular interaction between oxygen in DTPA-K_5 with Ba in $BaSO_4$. Intermolecular interaction of oxygen in DTPA-K_5 with barium occurs at r 3.25 with g(r) 2.68. Ma, *et al*. [43] previously studied that the intermolecular interaction DTPA-Na_5 demonstrates a closer interaction due to a shorter interaction radius between 001 $BaSO_4$ surface and O1 and O2 atoms in DTPA-Na_5 at 2.86 Å and 2.79 Å, respectively. Both of the O atoms are from the carboxylic group, which replaced both Na atoms. Figure 9 shows that the addition of synergist into the system reduced the g(r) value to 1.40. The usage of potassium carbonate as a synergist in the dissolution of barium sulphate using DTPA was previously suggested by Bageri, *et al*. [31]. The study shows that the addition of synergists into the DTPA-K_5 solution improves the dissolution of barium sulphate. Mahmoud, *et al*. [44] propose that K_2CO_3 will react directly with some of the $BaSO_4$ molecules forming $BaCO_3$, thus not improving the intermolecular interaction between oxygens in DTPA and barium atoms. In addition, the reduction of intermolecular interaction after the addition of synergists can be associated with the proximity effect of neighbouring atoms that reduce the intermolecular interaction with the increasing number of molecules [45, 46].

The initial and final configuration of molecules for DTPA-K_5 with $BaSO_4$ is shown in Figure 10 without synergist and Figure 11 with synergist. The addition of synergist (K_2CO_3) increases the number of molecules with potassium atoms dispersed out of the simulation box. The configuration shows no significant changes in the molecular dispersion of DTPA before and after simulation due to weak intermolecular interaction.

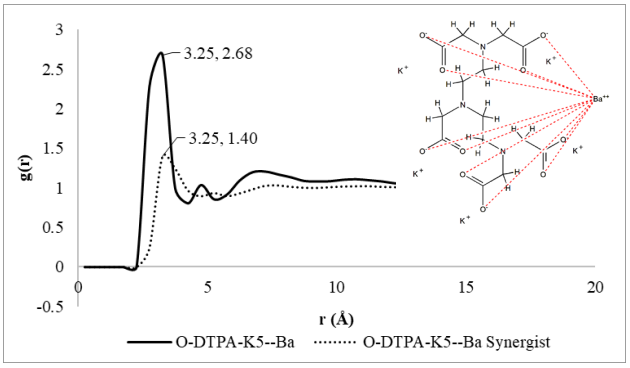

Figure 9 Intermolecular interaction of oxygen in DTPA-K_5 with Ba in $BaSO_4$ with and without synergist

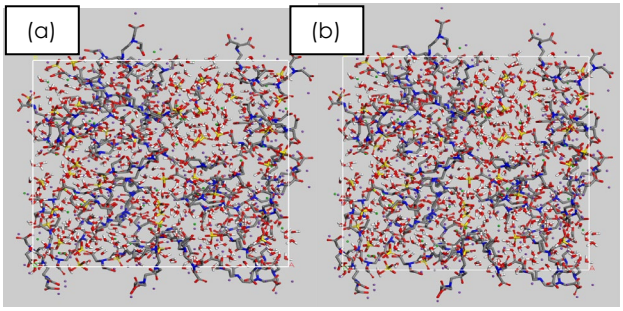

Figure 10 Initial (a) and final (b) configuration of molecules in DTPA-K_5—$BaSO_4$ system

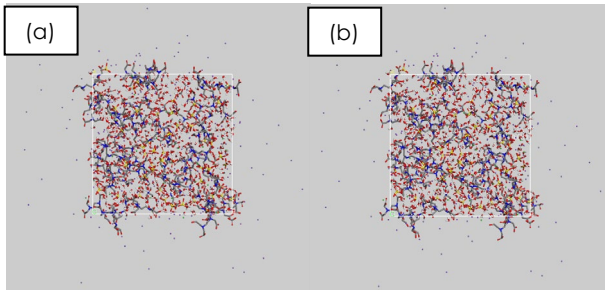

Figure 11 Initial (a) and final (b) configuration of molecules in DTPA-K_5—$BaSO_4$ with synergist system

3.2.1 Dissolution of Barium Sulphate with DTPA based dissolver

The effectiveness of the DTPA-K_5 chelate agent in dissolving $BaSO_4$ was evaluated. Figure 12 shows the dissolution of $BaSO_4$ in different concentrations of DTPA-K_5. $BaSO_4$ scale has a dense and hard crystal structure, and DTPA demonstrates a good solubility for $BaSO_4$ removal under strong alkaline conditions [43]. This study recorded the highest $BaSO_4$ dissolution at 0.6M of DTPA-K_5, with dissolution up to 30% at pH >12. At high concentrations of DTPA-K_5, the dissolution behaviour is influenced by the crowding of molecules at the barite surface, resulting in steric hindrance with a reduction in overall reaction activity [47]. A previous study reported that the solubility of barite is 1.17 g/L (650 ppm of Ba) in a 0.05 M DTPA solution during 19 hours at 22°C, indicating that a lower concentration of DTPA resulted in a good dissolving rate at a low temperature [48].

The addition of K_2CO_3 has further improved the dissolution capability, as shown in Figure 13. The solution with the addition of K_2CO_3 has a pH value of 13-14. The highest dissolution was recorded up to 40% for the addition of 5g of K_2CO_3 into 0.6 M DTPA-K_5 solution. The result also shows that $BaSO_4$ dissolved at a high alkalinity environment. High alkalinity allowed for full deprotonation of the chelate agent and increased the dissolution of $BaSO_4$ [30]. ICP-OES analysis shows that the concentration of Ba detected in the solution after the dissolution test was 8200 ppm. The increase in the dissolution rate of $BaSO_4$ with the addition of K_2CO_3 result is in agreement with the previous study by Bageri *et al*. in 2017 [31].

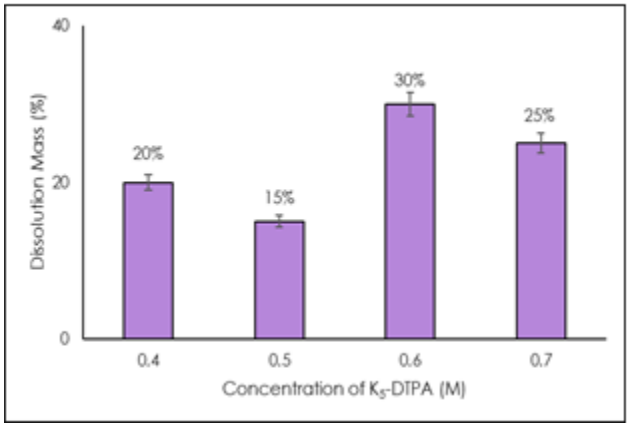

Figure 12 Dissolution of $BaSO_4$ in different concentrations of DTPA-K_5

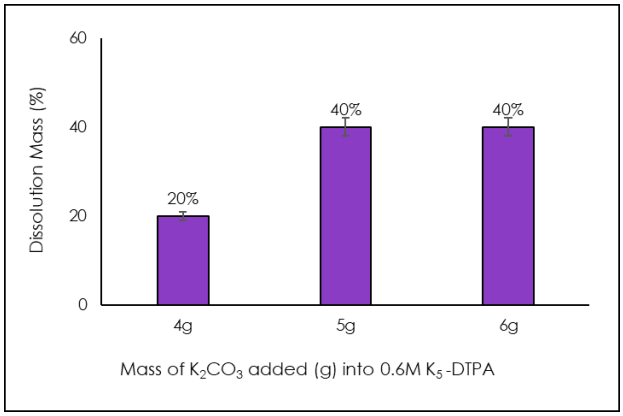

Figure 13 Dissolution of $BaSO_4$ in different mass (g) of DTPA-K_5 with potassium carbonate added

3.3 Intermolecular interaction of EDTA-Na_4 with Fe in FeS

Figure 14 shows the intermolecular interaction of EDTA-Na_4 with FeS. The delocalisation of COO- is expected to improve the intermolecular interaction due to the possibility of COO- groups forming a bond with Fe molecules [18, 49, 50]. The result shows that intermolecular interaction occurs at r 1.75 Å with a probability of 10.71. Previous study by Sulaiman, *et al*. [12] for intermolecular interaction of GLDA-Na_4 with FeS occurs at a similar r of 1.75 Å with a probability of slightly lower at g(r) of 10.17. This strong intermolecular interaction of iron in FeS with the chelating agent is also demonstrated by Che Azimi, *et al*. [17] for intermolecular interaction of DTPA with FeS.

However, the addition of synergist into the system shows insignificant changes in the intermolecular interaction between oxygen in EDTA-Na_4 with Fe with a slight reduction of probability from 10.71 to 10.01.

EDTA-Na_4 has a good intermolecular interaction with Fe that can be utilised as a dissolution agent. The initial and final configuration of molecules for EDTA-Na_4 with FeS is shown in Figure 15 without synergist and Figure 16 with synergist. Despite strong intermolecular interaction, the molecular conformation did not show any significant changes. However, the addition of synergist increases the number of molecules in the simulation box, which might cause the proximity effect, reducing the intermolecular interaction [45].

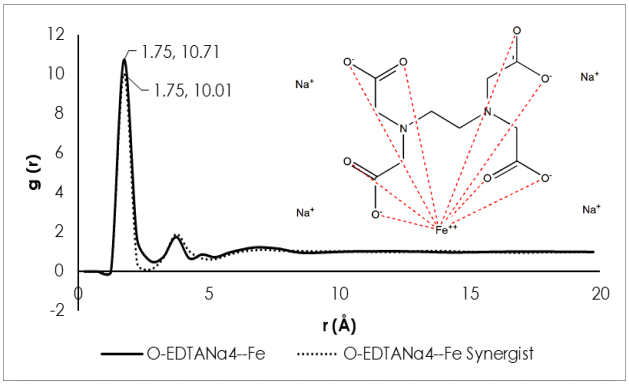

Figure 14 Intermolecular interaction of oxygen in EDTA-Na_4 with Fe

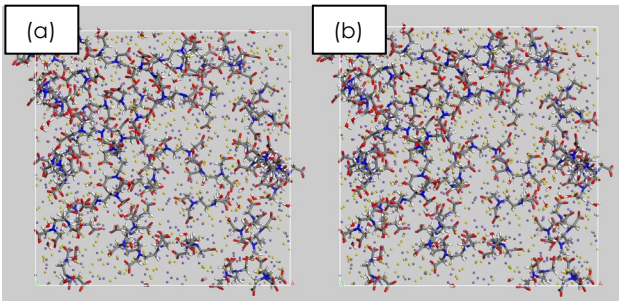

Figure 15 Initial (a) and final (b) configuration of molecules in the EDTA-Na_4-FeS system

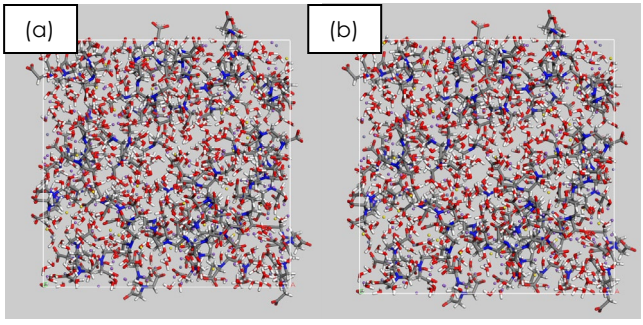

Figure 16 Initial (a) and final (b) configuration of molecules in EDTA-Na_4-FeS system with the synergist

3.3.1 Dissolution of FeS with EDTA-Based Dissolver

The dissolution test result for different concentrations of EDTA-Na_4 at 65 ° C and 24 hours is shown in Figure 17. The results indicated the same dissolution rate at 5% occurs at pH between 9 - 10.3, which exhibits alkaline properties. There was no significant improvement in FeS scale solubility at this pH range. Synergists such as potassium citrate and potassium chloride ranging at 2.5 wt. %, 5 wt. % and 10 wt. % used with Na_4-EDTA had no significant effect on the dissolution rates of FeS scale. This is because the pH of these two synergists at all different concentrations is in alkaline condition. Although previous studies using EDTA at pH 8-10 were able to dissolve 80 % of FeS scale after 20 hours [16], similar results could not be obtained in this study. Variation of solubility of FeS from the same source in similar dissolver concentration and condition was previously observed due to the effect of the molar ratio of FeS to acid as well as the presence of material such as grease that might block the dissolution of the metals on the surface of the solid scale [51].

Figure 18 shows the dissolution of FeS in 10 wt% of Na_4-EDTA with the addition of formic acid. The addition of formic acid reduces the pH from alkaline to acidic. The highest dissolution was recorded for the addition of 3 wt% of formic acid dissolved up to 25 % FeS at pH 4.4. ICP-OES analysis of the solvent after the dissolution shows the concentration of Fe detected at 3528 ppm. Addition of 1.5 wt. % hydrochloric acid, with a pH of 4.15, also showed a similar dissolution rate to formic acid at pH 4.41. At acidic conditions, the concentration of hydrogen (H^+) ions is high in the dissolver, which aids and speeds up the dissolution of the FeS scale. This is because scales such as iron (II) sulphide and carbonate depend on the brine pH [9]. The main mechanism of dissolution of FeS scale is visible at pH < 9, where H^+ attack is dominant [52].

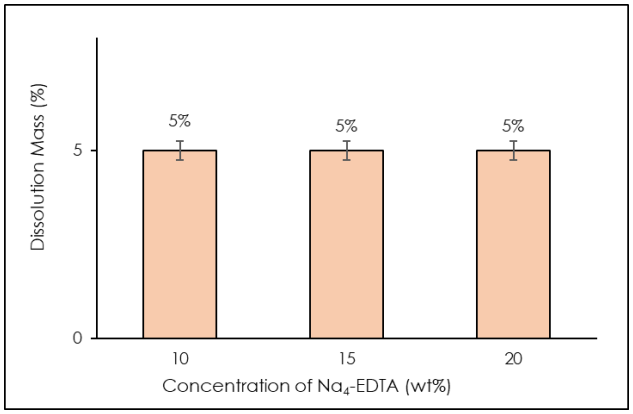

Figure 17 Dissolution of FeS in different concentrations of EDTA-Na_4

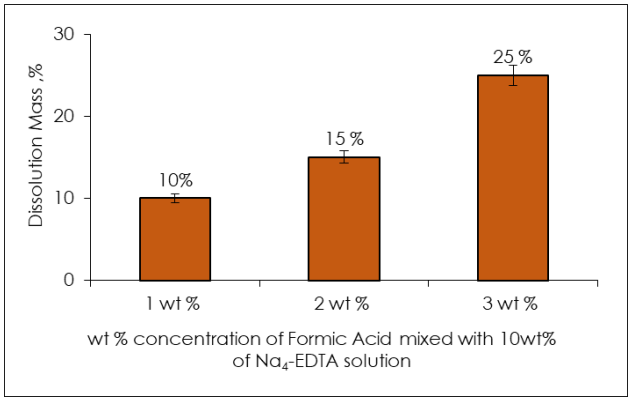

Figure 18 Dissolution of FeS in 10wt% of EDTA-Na_4 with different concentration of formic acid added (wt%)

3.3 Properties of Formulated Dissolver

Table 3 shows the properties of the final formulation for $CaCO_3$, $BaSO_4$, and FeS dissolver developed in this study. The corrosivity of carbon steel coupon in the final formulation for $CaCO_3$ dissolver is 18.0341 mpy at ambient temperature. This corrosivity rate, although high, is still considered good but needs to be used with caution as it still can damage steel surfaces for prolonged use [53]. However, further improvement can be done by adding a corrosion inhibitor to the formulation. For the dissolver of $BaSO_4$, this solution was found to be non-corrosive [53] at ambient temperature on carbon steel coupon measured at 0.09927 mpy. For dissolver of FeS, the final formulation is found to be corrosive on carbon steel coupon at ambient temperature measured at 90.78354 mpy. A corrosion inhibitor was recommended to improve this formulation further.

4.0 CONCLUSION

Fe with EDTA-Na_4 shows the highest intermolecular interaction, followed by Ca with EDTA-K_3 and Ba with DTPA-K_5. The addition of synergist slightly increased the intermolecular interaction of Ca with EDTA-K3 but showed no improvement of intermolecular interaction for Ba with DTPA-K_5 and Fe with EDTA-Na_4 when synergist was added. The combination of acetic acid in EDTA-K_3 significantly enhanced the removal of calcium carbonate by up to 59%. A combination of EDTA-K_3, HAc and HCl results in the highest dissolution of $CaCO_3$ at 68% or 19 940 ppm Ca. EDTA tend to precipitate at conditions below pH 4.88. Potassium carbonate is an effective synergist that can be mixed with DTPA-K5 for barium sulphate scale dissolution, giving 40% dissolution of $BaSO_4$ or 8200 ppm Ba. EDTA-Na_4 can be combined with formic acid to improve the FeS scale dissolution rate, with the highest dissolution rate of 25 % at a pH less than 5. It is recommended for the dissolution test to be conducted at several different concentrations to provide better data on the dissolution rate of solid scale in the formulation developed. The formulation for $CaCO_3$ and FeS was found to be corrosive; thus, a corrosion inhibitor was recommended for further improvement.

Table 3 Properties of formulated dissolver for $CaCO_3$, $BaSO_4$ and FeS

Properties			
Dissolver	EDTA-K_3+ HCl + HAc	DTPA-K_5+ K_2CO_3	EDTA-Na_4+ formic acid
Target Solid Scale	$CaCO_3$	BaSO4	FeS
Dissolution Capability (%)	68%,	40%	25%
Concentration of Metal ions Dissolved	19 940 ppm Ca	8200 ppm Ba	3528 ppm Fe
pH	4.87	13-14	4.4
Boiling point (°C)	101.1	104	101.2
Density (g/ml)	1.121	1.249	1.210
Corrosivity (mpy)	18.0341	0.09927	90.78354

Acknowledgement

This research is fully supported by Universiti Malaysia Pahang Al-Sultan Abdullah under UMPSA short-term grant RDU 170322, PGRS 170371 and technical support from Setegap Venture Petroleum.

Conflicts of Interest

The authors declare that there is no conflict of interest regarding the publication of this paper.

References

[1] M. Crabtree, D. Eslinger, P. Fletcher, M. Miller, A. Johnson, and G. King. 1999. Fighting Scale — Removal and Prevention. *Oilfield Review*. 11(3): 30–45. http://www.slb.com/~/media/Files/resources/oilfield_review/ors99/aut99/fighting.pdf.

[2] O. J. Vetter and W. A. Farone. 1987. Calcium Carbonate Scale in Oilfield Operations. *SPE Annual Technical Conference and Exhibition,* Dallas, Texas.

[3] A. A. Olajire. 2015. A Review of Oilfield Scale Management Technology for Oil and Gas Production. *Journal of Petroleum Science and Engineering*. 135: 723–737. Doi: 10.1016/j.petrol.2015.09.011.

[4] A. Singha and M. A. Quraishi. 2015. Acidizing Corrosion Inhibitors: A Review. *Journal of Materials and Environmental Science*. 6(1): 224–235.

[5] P. Rajeev, A. O. Surendranathan, and C. S. N. Murthy. 2012. Corrosion Mitigation of the Oil Well Steels using Organic Inhibitors-A Review. *Journal of Materials and Environmental Science*. 3(5): 856–869.

[6] H. A. Nasr-El-Din and A. Y. Al-Humaidan. 2001. Iron Sulfide Scale: Formation, Removal and Prevention. *SPE International Symposium on Oilfield Scale Aberdeen,* United Kingdom. 30–31 January. https://www.onepetro.org/conference-paper/SPE-68315-MS.

[7] T. Chen, Q. Wang, F. F. Chang, and Y. T. Al-Janabi. 2016. New Developments in Iron Sulfide Scale Dissolvers. Paper Presented at *CORROSION 2016*, NACE International, Houston, TX, 2016.

[8] J. J. Wylde and C. O. Services. 2014. Sulfide Scale Control in Produced Water Handling and Injection Systems: Best Practices and Global Experience Overview. Aberdeen, Scotland, 2014.

[9] H. Gamal, S. Elkatatny, D. Al Shehri, and M. Bahgat. 2020. A Novel Low-Temperature Non-Corrosive Sulfate/Sulfide Scale Dissolver. *Sustainability*. 12(6). Doi: 10.3390/su12062455.

[10] M. A. Mahmoud, H. A. Nasr-El-Din, C. A. De Wolf, J. N. LePage, and J. H. Bemelaar. 2011. Evaluation of a New Environmentally Friendly Chelating Agent for High-Temperature Applications. *SPE Journal*. 16(3): 559–574. Doi: Doi 10.2118/127923-Pa.

[11] M. H. Sulaiman, F. Adam, Z. Yaacob, and Z. Mohd Noor. 2020. Synthesis of Ionic Salt for Calcite and Barite Solid Scale Dissolution. *IOP Conference Series: Materials Science and Engineering*. 736(2): 1–7. Doi: 10.1088/1757-899x/736/2/022022.

[12] M. H. Sulaiman, F. Adam, Z. Yaacob, M. Z. Sujak, and Z. Mohd Noor. 2020. Intermolecular Interaction of Carboxylic Group with Calcium Ions and Dissolution of Solid Scales in Bmim-PF6 and Tba-NfO Ionic Liquid Solution. *Malaysian Journal of Microscopy*. 16(1): 205–216.

[13] C. C. Okwuwa, F. Adam, F. Mohd Said, and M. E. Ries. 2023. Cellulose Dissolution for Edible Biocomposites in Deep Eutectic Solvents: A Review. *Journal of Cleaner Production*. Doi: 10.1016/j.jclepro.2023.139166.

[14] M. H. Al-Khaldi, A. M. Al-Juhani, S. H. Al-Mutairi, and M. N. Gurmen. 2011. New Insights into the Removal of Calcium Sulfate Scale. Paper SPE-144158-MS, presented at the SPE European Formation Damage Conference, Noordwijk, Netherlands, June 7–10. https://doi.org/10.2118/144158-MS.

[15] T. Almubarak, J. H. Ng, R. Ramanathan, and H. A. Nasr-El-Din. 2021. Chelating Agents for Oilfield Stimulation: Lessons Learned and Future Outlook. *Journal of Petroleum Science and Engineering*. 205. Doi: 10.1016/j.petrol.2021.108832.

[16] T. Almubarak, J. H. Ng, R. Ramanathan, and H. A. Nasr-El-Din. 2021. Chelating Agents for Oilfield Stimulation: Lessons Learned and Future Outlook. *Journal of Petroleum Science and Engineering*. 205. Doi: 10.1016/j.petrol.2021.108832.

[17] A. Z. Che Azimi, N. Abdullah, and F. Adam. 2024. Molecular Dynamic Simulation of DTPA with $CaCO_3$ and FeS. *Malaysian Journal of Analytical Sciences*. 28(4): 956–974.

[18] M. H. Sulaiman, F. Adam, Z. Yaacob, M. Z. Mohd Noor, and N. Abdullah. 2022. Evaluation of Carboxylic Acid and Amine Groups with $CaCO_3$, FeS and $BaSO_4$: Molecular Dynamic Simulations and Experimental Study. *Arabian Journal for Science and Engineering*. 47(5): 6693–6706. Doi: 10.1007/s13369-022-06647-2.

[19] A. R. Leach, *Molecular Modelling: Principles and Applications*. New Jersey: Prentice Hall, 2001.

[20] X. Yu, Y. Wu, J. Wang, and J. Ulrich. 2018. Experimental Assessment and Modeling of the Solubility of Malonic Acid in Different Solvents. *Chemical Engineering & Technology*. 1–11. Doi: 10.1002/ceat.201700227.

[21] Julia Burdge and Jason Overby. 2020. *Chemistry: Atoms First*. 4th ed. New York: McGraw Hill.

[22] N. Shahrir *et al.* 2022. The Role of Solvent Hydroxyl Functional Groups on the Interaction Energy and Growth of Form I Paracetamol Crystal Facets. *Organic Process Research & Development*. 26(12): 3226–3235. Doi: 10.1021/acs.oprd.2c00151.

[23] Royal Society of Chemistry. 2025. Edetate Sodium. *ChemSpider*. Accessed January 10, 2025. https://www.chemspider.com/Chemical-Structure.5914.html.

[24] S. K. Abdul Mudalip, F. Adam, and M. R. Abu Bakar. 2019. Evaluation of the Intermolecular Interactions and Polymorphism of Mefenamic Acid Crystals in N,N-dimethyl Formamide Solution: A Molecular Dynamics Simulation and Experimental Study. *Comptes Rendus Chimie*. 22(11–12): 771–778. Doi: 10.1016/j.crci.2019.08.005.

[25] S. K. A. Mudalip, M. R. Abu Bakar, P. Jamal, F. Adam, and Z. M. Alam. 2016. Molecular Recognition and Solubility of Mefenamic Acid in Water. *Asian Journal of Chemistr*. 28(4): 853–858. Doi: 10.14233/ajchem.2016.19538.

[26] G. Schwarzenbach.1952. "Der Chelateffekt," *Helvetica Chimica Acta*. 35(7): 2344–2359. Doi: https://doi.org/10.1002/hlca.19520350721.

[27] F. Adam, A. B. Siti Hana, M. M. Yusoff, and S. N. Tajuddin. 2014. Molecular Dynamic Simulation of the Patchouli Oil Extraction Process. *Journal of Chemical & Engineering Data*. 59(2): 183–188. Doi: 10.1021/je3013292.

[28] L. N. Plummer and E. Busenberg. 1982. The Solubilities of Calcite, Aragonite and Vaterite in CO_2-H_2O Solutions between 0 and 90°C, and an Evaluation of the Aqueous Model for the System $CaCO_3$-CO_2-H_2O. *Geochimica et Cosmochimica Acta*. 46(6): 1011–1040. Doi: https://doi.org/10.1016/0016-7037(82)90056-4.

[29] N. Kallay, V. Tomašić, S. Žalac, and L. Brečević. 1997. Calorimetric Investigation of Kinetics of Solid Phase Dissolution: Calcium Carbonate Dissolution in Aqueous EDTA Solution. *Journal of Colloid and Interface Science*. 188(1): 68–74. Doi: 10.1006/jcis.1996.4729.

[30] B. S. Bageri, M. A. Mahmoud, R. A. Shawabkeh, and A. Abdulraheem. 2017. Evaluation of Barium Sulfate (Barite) Solubility Using Different Chelating Agents at a High Temperature. *Journal of Petroleum Science and Technology*. 7(1): 42–56. Doi: 10.22078/JPST.2017.707.

[31] B. S. Bageri, M. A. Mahmoud, R. A. Shawabkeh, S. H. Al-Mutairi, and A. Abdulraheem. 2017. Toward a Complete Removal of Barite (Barium Sulfate $BaSO_4$) Scale Using Chelating Agents and Catalysts. *Arabian Journal for Science and Engineering*. 42(4): 1667–1674. Doi: 10.1007/s13369-017-2417-2.

[32] K. Dunn and T. F. Yen. 1999. Dissolution of Barium Sulfate Scale Deposits by Chelating Agents. *Environmental Science & Technology*. 33(16): 2821–2824. Doi: 10.1021/es980968j.

[33] W. W. Frenier, D. Wilson, D. Crump, and L. Jones. 2000. Use of Highly Acid-Soluble Chelating Agents in Well Stimulation Services. *SPE Annual Technical Conference and Exhibition*, Dallas, Texas, 1–4 October.

[34] J. Moghadasi, H. Müller-Steinhagen, M. Jamialahmadi, and A. Sharif. 2007. Scale Deposits in Porous Media and Their Removal by Edta Injection. *Heat Exchanger Fouling and Cleaning VII*. 59–60. http://dc.engconfintl.org/heatexchanger2007/10.

[35] A. Z. Che Azimi, N. Abdullah, F. Adam, Z. Hassan, S. Abdul Rahman, and M. Z. Mohd Noor. 2022. The Simulation of Intermolecular Interactions of Carboxylic and Amine Groups with Calcium Carbonate. *Jurnal Teknologi*. 85(1): 91–98. Doi: 10.11113/jurnalteknologi.v85.18589.

[36] International Organization of Legal Metrology (OIML). 2011. Density Measurement.

[37] E. R. Squibb. 1897. Note On an Improved Specific Gravity Bottle or Pyknometer. *Journal of the American Chemical Society*. 19(2): 111–114. Doi: 10.1021/ja02076a004.

[38] A. Siwoloboff. 1886. Ueber die Siedepunktbestimmung kleiner Mengen Flüssigkeiten. 19(1): 795–796. Doi: 10.1002/cber.188601901181.

[39] S. Munir, M. H. Pelletier, and W. R. Walsh. 2016. Potentiodynamic Corrosion Testing. *J Vis Exp*. 115. Doi: 10.3791/54351.

[40] F. Adam. 2012. An Examination into the Influence and Change of Solution Structure on the Polymorphic Behaviour of 2,6-Dihydroxybenzoic Acid. PhD Thesis. University of Leeds, Leeds.

[41] L. Li, H. Nasr-El-Din, F. Chang, and T. Lindvig. 2008. Reaction of Simple Organic Acids and Chelating Agents with Calcite. *Proceedings of International Petroleum Technology Conference*.

[42] J. N. Lepage, C. A. De Wolf, J. H. Bemelaar, and H. A. Nasr-El-Din. 2011. An Environmentally Friendly Stimulation Fluid for High-Temperature Applications. *SPE Journal*. 16(1): 104–110. Doi: doi.org/10.2118/121709-PA.

[43] C. Ma, X. Liu, C. Wang, S. Gao, and X. Huang. 2023. Preparation of Barium Sulfate Chelating Agent DTPA-5Na and Molecular Dynamics Simulation of Chelating Mechanism. *RSC Adv*. 13(49): 34455–34463. Doi: 10.1039/d3ra05564g.

[44] M. Mahmoud *et al.* 2018. Evaluation of the Reaction Kinetics of Diethylenetriaminepentaacetic Acid Chelating Agent and a Converter with Barium Sulfate (Barite) Using a Rotating Disk Apparatus. *Energ Fuel*. 32(9): 9813–9821. Doi: 10.1021/acs.energyfuels.8b02332.

[45] U. Becker, K. M. Rosso, and M. F. Hochella. 2001. The Proximity Effect on Semiconducting Mineral Surfaces: A New Aspect of Mineral Surface Reactivity and surface Complexation Theory? *Geochimica et Cosmochimica Acta*. 65(16): 2641–2649. Doi: 10.1016/s0016-7037(01)00624-x.

[46] C. V. Putnis, M. Kowacz, and A. Putnis. 2008. The Mechanism and Kinetics of DTPA-promoted Dissolution of Barite. *Applied*

Geochemistry. 23(9): 2778–2788. Doi: 10.1016/j.apgeochem.2008.07.006.

[47] A. Putnis, C. V. Putnis, and J. M. Paul. 1995. The Efficiency of a DTPA-Based Solvent in the Dissolution of Barium Sulfate Scale Deposits. Paper 57597, presented at the *SPE International Conference on Oilfield Chemistry* (95OCS). Society of Petroleum Engineers.

[48] R. D. Sosa *et al.* 2020. Acidic Polysaccharides as Green Alternatives for Barite Scale Dissolution. *ACS Appl Mater Interfaces*. 12(49): 55434–55443. Doi: 10.1021/acsami.0c16653.

[49] D. Braga, J. J. Novoa, and F. Grepioni. 2001. On the Charge Delocalisation in Partially Deprotonated Polycarboxylic Acid Anions and Zwitterions Forming (−)O–H···O(−) Interactions in the Solid State. *New Journal of Chemistry*. 25(2): 226–230. Doi: 10.1039/b005235n.

[50] W. Sailer *et al.* 2003. Dissociative Electron Attachment to Acetic Acid (CH3COOH). *Chemical Physics Letters*. 378(3–4): 250–256. Doi: 10.1016/s0009-2614(03)01285-5.

[51] H. A. Nasr-El-Din and A. Y. Al-Humaidan. 2001. Iron Sulfide Scale: Formation, Removal and Prevention. Paper SPE-68315-MS, presented at the *SPE International Symposium on Oilfield Scale*, Aberdeen, United Kingdom, January 30–31. Society of Petroleum Engineers. https://www.onepetro.org/conference-paper/SPE-68315-MS.

[52] R. Ramanathan and H. Nasr-El-Din. 2019. Evaluation of Chelating Agents for Iron Sulfide FeS Scale Removal. *Abu Dhabi International Petroleum Exhibition & Conference*, Abu Dhabi, UAE, 11–14 November 2019. Paper SPE-197891-MS. Society of Petroleum Engineers.

[53] N. Saxena, S. Kumar, M. K. Sharma, and S. P. Mathur. 2013. Corrosion Inhibition of Mild Steel in Nitric Acid Media by some Schiff Bases Derived from Anisalidine. *Polish Journal of Chemical Technology*. 15(1): 61–67. Doi: 10.2478/pjct-2013-0011.